Macromolecular Research, Vol. 17, No. 12, pp 995-1002 (2009)

Luminescent Polynorbornene/Quantum Dot Composite Nanorods and Nanotubes Prepared from AAO Membrane Templates

Sewon Oh, Young Hyun Cho, and Kookheon Char*

School of Chemical and Biological Engineering, Center for Functional Polymer Thin Films, Seoul National University, Seoul 151-744, Korea

Received April 14, 2009; Revised May 14, 2009; Accepted June 17, 2009

Abstract: Luminescent polynorbornene (PNB)/quantum dot (CdSe@ZnS; QD) composite nanorods and nanotubes were successfully prepared using anodic aluminum oxide (AAO) membranes of various pore sizes as templates. To protect QDs with high quantum yield from quenching during the phosphoric acid treatment used to remove the AAO templates, chemically stable and optically clear norbornene-maleic anhydride copolymers (P(NB-*r*-MA)) were employed as a capping agent for QDs. The amine-terminated QDs reacted with maleic anhydride moieties in P(NB-*r*-MA) to form PNB-grafted QDs. The chemical- and photo-stability of QDs encapsulated with PNB copolymers were investigated by photoluminescence (PL) spectroscopy. By varying the pore size of the AAO templates from 40 to 380 nm, PNB/QD composite nanorods or nanotubes were obtained with a good dispersion of QDs in the PNB matrix.

Keywords: norbornene-maleic anhydride copolymer, quantum dot (QD), anodic aluminum oxide (AAO), luminescent, nanorod, nanotube.

Introduction

Quantum dots (QDs) recently received enormous attention due to their broad range of potential applications in light emitting diodes,[1-4] lasers,[5-7] photovoltaic devices,[8,9] as well as biomarkers[10-12] whose unique optical properties depend on their size, which is referred to as the quantum confinement effect.[13-15] The stability of highly luminescent nanocrystals (NCs) has been one of the most promising paths for successful application of QDs in practical setting. NCs with superb optical properties have been achieved through the passivation of NC surface using organic or inorganic overlayers.[16-22] Many proposed applications of QDs require the nanoparticles to be well-dispersed in a polymer matrix.[23] Unfortunately, the problem of particle agglomeration is often encountered when these nanoparticles are used during practical operations. Consequently, nanoparticles (such as QDs) well dispersed in a host material are highly desirable for practical applications.[24] In particular, one-dimensional (1-D) nanostructure consisting of QDs possesses useful optical properties possibly applicable in areas such as optical devices and DNA sensing.[25-27]

In order to prepare such 1-D nanostructures, template-based method, layer-by-layer deposition method, and self-assembly method have been employed.[28-31] Particularly, the porous membrane-mediated method (template-based method) has several advantages in obtaining 1-D nanocomposites.[32] The well-defined size, orientation, and confinement of porous structures make it possible to introduce host materials into tailored positions.[33,34] However, it still remains as a challenge to develop a facile and novel preparation method for 1-D nanocomposite materials. Recently, we have developed a fabrication method to yield chemically stable and optically clear polymer/QD composite nanorods or nanotubes prepared from anodic aluminum oxide (AAO) membranes with well-ordered and nanometer-sized channels.

In the present study, we report a novel fabrication method for luminescent polynorbornene (PNB)/QD composite nanorods or nanotubes based on AAO membranes of different pore size. Amine-functionalized CdSe@ZnS QDs were attached to norbornene copolymer main chains by reaction with maleic anhydride moieties in the copolymer. Norbornene copolymers, as chemically stable and optically clear capping agents, could protect QDs from quenching during the AAO etching process. Finally, we obtained polymer/QD composite nanorods and nanotubes of different size using AAO templates with pore size ranging from 40 to 380 nm. Although polymer nanorods or nanotubes based on AAO membranes have previously been reported,[35] no systematic study on chemically stable and luminescent polymer/QD composite nanorods or nanotubes has yet to be performed in detail, which is the main objective of the present study.

*Corresponding Author. E-mail: khchar@plaza.snu.ac.kr

Experimental

Materials. For the synthesis of norbornene-maleic anhydride copolymer (P(NB-*r*-MA)), 2,3-bicyclo[2.2.1]hept-2-ene (or norbornene, NB) was dried over calcium hydride and purified by distillation. Maleic anhydride was used as received. Azobisisobutyronitrile (AIBN) was used after recrystallization. Anhydrous THF was used as a reaction solvent. All the reagents for the synthesis of P(NB-*r*-MA) were purchased from Aldrich. High purity (99.999%) aluminum foils for the preparation of anodized aluminum oxide (AAO) membrane were purchased from Goodfellow. Phosphoric acid (85%), perchloric acid (70%), and oxalic acid (98%) were purchased from Sigma Aldrich. Cadmium oxide (CdO, 99.99%), zinc acetate ($Zn(acet)_2$, 99.9%, powder), selenium (Se, 99%, powder), sulfur (S, 99.9%, powder), tributylphosphine (TBP, 90%), oleic acid (OA, 90%), cysteamine hydrochloride (CAm, 98%), and 1-octadecene (1-ODE, 90%) for the synthesis of CdSe @ZnS QDs were used as received from Aldrich. 9,10-Diphenylanthracene (99%) was purchased from Fluka.

Synthesis of Norbornene-Maleic Anhydride Copolymers (P(NB-*r*-MA)). Norbornene monomer was polymerized by radical polymerization in the presence of maleic anhydride to yield norbornene-maleic anhydride copolymer (P(NB-*r*-MA)). 1:1 Molar ratio of norbornene (10 g, 0.106 mol) and maleic anhydride (10.38 g, 0.106 mol) were dissolved in 100 mL of dry THF and a catalytic amount of AIBN (0.174 g, 0.00106 mol) was added to the mixture. The reaction flask was well stirred until most of solid materials dissolved and then was degassed three times by the freeze-thaw method. The reaction mixture was refluxed overnight for 24 h at 60 °C. After 24 h, the reaction mixture was cooled down to room temperature to finish the polymerization. The polymer product was precipitated by pouring the solution into *n*-hexane. The precipitated white norbornene copolymer was collected by suction filtration and dried in a vacuum oven. The copolymerization yielded an alternating copolymer. 1:1 Stoichiometry of norbornene to maleic anhydride was proven by ^{1}H NMR. ^{1}H NMR (TDF): 4.3-2.9 (br m, 2H of maleic anhydride), and 3.0-0.7 (br m, 10H, cycloaliphatic of norbornene copolymer). ^{13}C NMR (TDF): 175-171 (br m, 2C, carbonyl carbon of maleic anhydride). The weight-average molecular weight (M_w) was determined to be 15,900 g/mol with PDI of 1.48.

Synthesis of CdSe@ZnS Nanocrystals. CdSe@ZnS QDs were prepared by the synthetic scheme previously reported.[36] As a typical synthetic procedure, 0.2 mmol of CdO, 4 mmol of $Zn(acet)_2$, and 5 mL of oleic acid (OA) were placed in a 100 mL round flask, heated to 150 °C and degassed under 100 mtorr pressure for 20 min to obtain a mixture of $Cd(OA)_2$ and $Zn(OA)_2$. The reactor was then filled with N_2 gas, added with 15 mL of 1-octadecene and further heated to 300 °C to form a clear mixture solution of $Cd(OA)_2$ and $Zn(OA)_2$. At this temperature, a mixed solution of 0.1 mmol of Se and 4 mmol of S in 2 mL of trioctylphosphine (TOP) was quickly injected into the reaction flask. The reaction mixture was allowed for reaction at the elevated temperature for 10 min to yield CdSe@ZnS QDs. The synthesized QDs were cooled to room temperature, purified by adding 20 mL of toluene and 30 mL of ethanol and finally dispersed in chloroform. For the encapsulation of QDs with norbornene-maleic anhydride copolymers, the surface of prepared QDs, initially capped with OA, was further treated with cysteamine (CAm) and dispersed in water (pH 6) after repeated purification step with water and acetone to yield amine-functionalized QDs. The PL emission spectrum of prepared QDs was measured by an ACTON spectrometer.

Preparation of Anodized Aluminum Oxide (AAO) Membranes. Hexagonally ordered porous alumina templates were prepared based on the two-step anodization process reported by Masuda *et al.*.[37,38] An aluminum foil was degreased in acetone to remove organic impurities and located on a copper plate, acting as the anode. One side (with a circular area of 1 cm in diameter) of the aluminum foil was exposed to an electrolyte solution in a thermally insulated cell. Three types of electrolytes (sulfuric, oxalic, and phosphoric acid) were used to prepare AAO membranes with relevant pore size used in this study. The temperature of electrolyte solution was maintained constant 100 °C in sulfuric acid, 17 °C in oxalic acid, and 0 °C in phosphoric acid during the anodization process. The exposed side of an aluminum foil was first electropolished in a $HClO_4/C_2H_5OH$ (1:3 by volume) mixture solution. After the electropolishing of the aluminum foil, first anodization process was conducted under constant voltage (at 25 V in sulfuric acid, at 40 V in oxalic acid, and 195 V in phosphoric acid) using a power supply (Agilent Technologies N5700) for 3 to 12 h. The concentration of electrolytes used for the anodization is 0.3 M in sulfuric acid, 0.3 M in oxalic acid, and 1 wt% in phosphoric acid, respectively. Subsequently, the aluminum oxide layer was removed by chemical etching in a mixture solution of phosphoric acid (6 wt%) and chromic acid (1.8 wt%) with gentle stirring at 45 °C for more than 7 h. The remaining well-ordered periodic concave patterns on the aluminum substrate play a role as pore nucleation centers for the following anodization step. The second anodization was conducted under the same condition as the first anodization. After the second anodization, prepared samples were washed with plenty amount of deionized water, isopropyl alcohol, and acetone. The bottom aluminum part was removed in a $CuCl_2$/HCl mixture solution. By varying the experimental parameters such as type of electrolyte, temperature, and applied voltage power, the pore diameter of anodic aluminum oxides can be controlled from 40 to 200 nm. Additionally, for further expansion of the pore diameter in anodic aluminum oxide membranes, we have employed the wet-chemical etching process. The depth of pores in the AAO membranes can be adjusted by anodization time during the

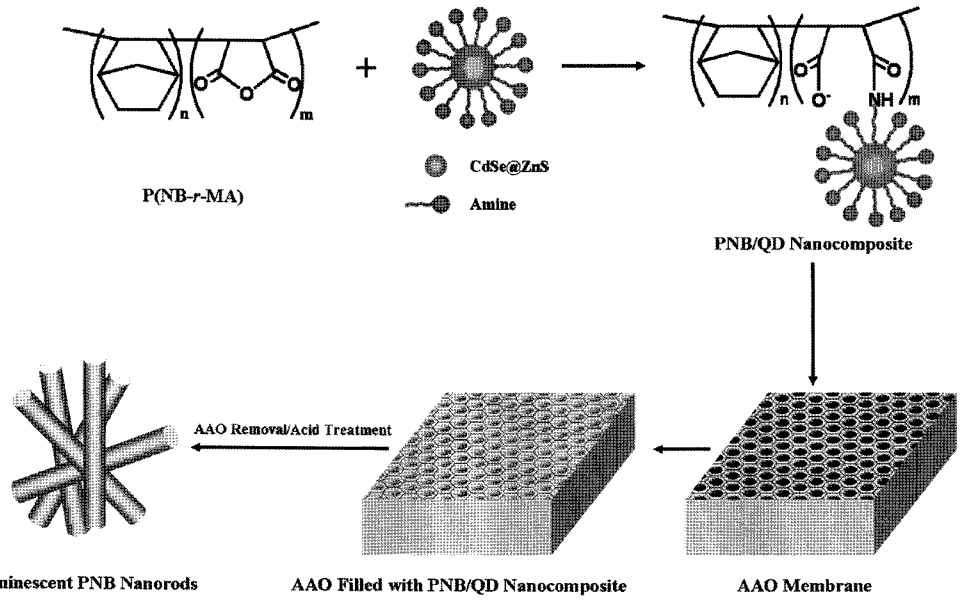

Scheme I. Schematic on the preparation of luminescent PNB/QD composite nanorods.

second anodization process.

Preparation of PNB/QD Composite Nanorods and Nanotubes. The maleic anhydride moieties in the norbornene-maleic anhydride copolymers can readily react with amine groups sticking out from QDs under mild condition. Scheme I represents a process flow for the preparation of PNB/QD composite nanorods. 0.5 g of P(NB-*r*-MA) was dissolved in THF at 1 wt% solution. A 0.1 mL of amine-functionalized CdSe@ZnS QD solution (at 5 wt% water solution) was then added to the P(NB-*r*-MA) solution. After 30 min of reaction, the reaction mixture (PNB/QD composites) was placed on an AAO membrane surface for 10 min. The AAO membrane templates were removed by treatment with phosphoric acid (10 wt%) at 45 °C for 1 h. Finally, PNB/QD composite nanorods and nanotubes were obtained without significant loss of the quantum efficiency of CdSe@ZnS QDs.

Photostability Test of CdSe@ZnS Quantum Dots. To compare the photo- and chemical-stability of CdSe@ZnS QDs as prepared with QDs grafted with PNB chains during the AAO etching process, each solution was treated with phosphoric acid (10 wt%) for 1 h. The quantum efficiency of each sample was measured by PL spectroscopy before and after the treatment with phosphoric acid. The output from a home-built cavity-dumped mode-locked Ti:sapphire laser (740 nm, 500 kHz, 20 fs) was doubled to 350 nm with a 100 μm thick BBO crystal for the excitation of CdSe@ZnS QDs. A lens (f= 150 mm) and a parabolic mirror (f= 101.6 mm) were used to focus the excitation light and to collect PL in the backscattering geometry, respectively. PL spectra were obtained with a TE-cooled CCD (Andor, DU-401) mounted on a 30 cm monochromator (Acton, SP-300, 150 grooves/mm) with 2 nm resolution. The instrument response function was 50 ps (FWHM), yielding 10 ps time resolution with deconvolution.

Characterization. ^{1}H NMR spectra were obtained at room temperature using a Bruker (Avance 500 MHz). Gel permeation chromatographic (GPC) analyses were carried out using a Waters Alliance GPC 450 Systems. Chloroform was used as an eluent at a flow rate of 1.0 mL/min and the GPC data were calibrated based on PS standards, ranging from 500 to 1,000,000 in molecular weight. Fourier transformed infrared spectroscopy (FTIR) measurements were made on a JASCO FT/IR 200 spectrometer; 16 accumulations were signal-averaged at a resolution of 4 cm^{-1}. FTIR spectrum was obtained for each film placed on a Si wafer in transmission mode at room temperature. Morphologies of PNB/QD composite nanorods were obtained with field-emission scanning electron microscopy (FE-SEM, JEOL 7401F). Transmission electron microscopy (TEM) was also performed on a JEM-2000EXII microscope. Photoluminescence (PL) spectra were collected on an ACTON spectrometer. Photoluminescent quantum yield (PL QY) of the QDs used in this study was measured and estimated by comparing its fluorescence intensity with the intensity of primary standard dye solutions (9,10-diphenylanthracene, QY=91% in ethanol) at the same optical density (0.05) and at the same excitation wavelength (350 nm).

Results and Discussion

Synthesis of Norbornene-Maleic Anhydride Copolymers (P(NB-*r*-MA)). Norbornene can be commonly polymerized by three different mechanisms: ring-opening metathesis polymerization (ROMP),[39] cationic polymerization,[40] and vinyl addition polymerization.[41-44] Among these polymerization mechanisms, vinyl polymerized norbornene copolymers are

highly interesting due to their excellent physical and chemical properties such as high glass transition temperature, high optical transparency, low dielectric constant, and excellent chemical resistance.[45] However, these intrinsic properties could be sometimes major drawbacks as their inherent brittle character and poor solubility in common organic solvents significantly limits its potential applications. Recently, it has been shown that these intrinsic drawbacks are easily overcome through the introduction of various functional groups to the PNB main backbone.[46,47] However, it is not still easy to introduce such functional moieties to the PNB main chains due to the steric hindrance as well as the catalytic deactivation during polymerization reaction. Consequently, in order to improve the intrinsic physical properties of norbornene-based copolymers, we copolymerized norbornene with highly reactive maleic anhydride based on radical polymerization that, in turn, can readily form a complex with amine-terminated nanomaterials. Radically polymerized P(NB-*r*-MA) was prepared by the freeze-evacuate-thaw method to remove oxygen from the reaction environment. Norbornene and maleic anhydride were polymerized with alternating sequence since the multiplication of reactivity ratios (r_{nb} and r_{ma}) is close to zero. The incorporated monomer ratios, estimated from ^{1}H NMR data, were thus 50 and 50 mol% for norbornene and maleic anhydride, respectively. Moreover, the peaks indicating double bonds in norbornene and maleic anhydride (δ 6.2~5.9 and δ 7.2~7.0, respectively) completely disappeared after the polymerization. From the ^{13}C NMR spectra, the peak at δ 174-170 is assigned to the carbonyl carbon of maleic anhydride (see Figure 1).

Analysis of Structural Changes of P(NB-*r*-MA) upon Association with QDs. To prepare luminescent PNB/QD composite nanorods and nanotubes, we mixed the P(NB-*r*-MA) solution with CdSe@ZnS QDs. The maleic anhydride moieties in the P(NB-*r*-MA) copolymer readily react with amine-terminated CdSe@ZnS QDs. In order to check if the

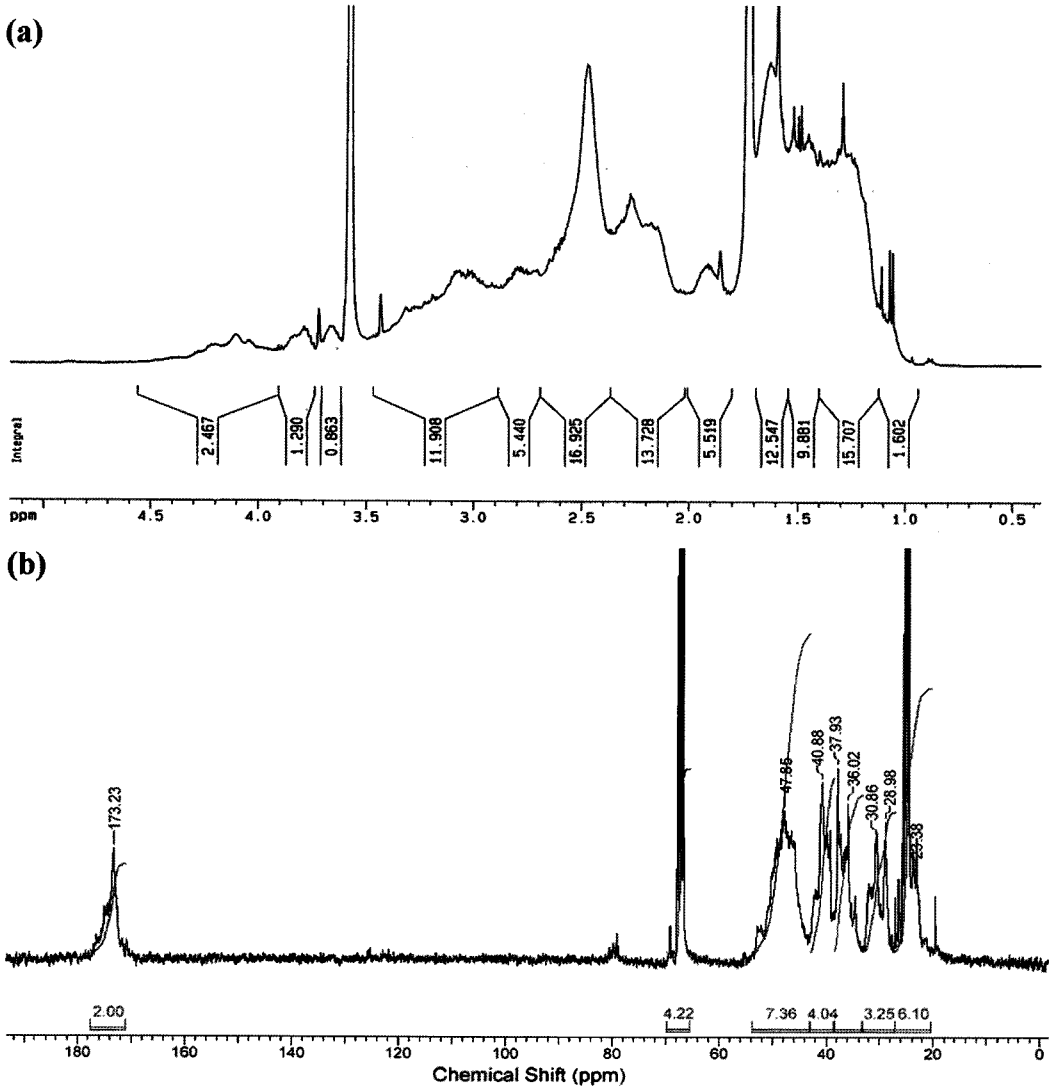

Figure 1. (a) ^{1}H NMR data and (b) ^{13}C NMR data of P(NB-*r*-MA).

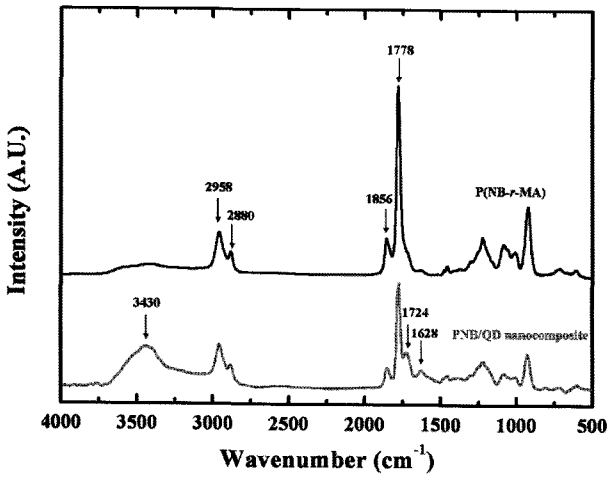

Figure 2. FTIR spectra showing the structural change of P(NB-*r*-MA) before and after the addition of amine-functionalized CdSe @ZnS.

amine-terminated groups originating from QDs chemically bind to maleic anhydride groups in the P(NB-*r*-MA) copolymer, the structural change in maleic anhydride was monitored by IR measurments, as shown in Figure 2. The intense peaks around 2700~3200 cm^{-1} are assigned to sp^2 CH stretching peaks from the PNB main chains. It is noted that these peaks do not change during the reaction with QDs. The two peaks around 1856 and 1778 cm^{-1} are assigned to C=O asymmetric and symmetric stretching originating from MA, respectively. After the association or reaction of amine-terminated QDs with P(NB-*r*-MA) copolymer, two new peaks emerge at 1724 and 1630 cm^{-1} and were assigned to the C=O stretching vibration of carboxylic acid and amide, respectively. Interestingly, the peaks at 1856 and 1778 cm^{-1} from MA drastically decrease almost simultaneously when the two new peaks at 1724 and 1630 cm^{-1} start to appear. And the broad peak at 3430 cm^{-1} is assigned to the -NH- and NH_2 stretching peak from amine-terminated QDs. These spectroscopic evidences support that CdSe@ZnS QDs form nanocomposites with grafted norbornene-maleic anhydride copolymers.

Chemical- and Photo-Stability of CdSe@ZnS QDs Grafted with P(NB-*r*-MA). To check the effect of AAO removal (or etching) process on the chemical- and photo-stability of CdSe@ZnS QDs and QDs grafted with P(NB-*r*-MA) copolymers, we added the identical amount of phosphoric acid, used as an etching solution, to pristine QDs as well as PNB/QD nanocomposite solutions. Figure 3(a) shows the PL emission spectra of CdSe@ZnS QDs before and after the phosphoric acid treatment. The emission wavelength ($\lambda_{max.}$) of pristine CdSe@ZnS QDs is 506 nm. The photoluminescent quantum yields (PL QY (Φ)) of pristine QDs and QDs grafted with P(NB-*r*-MA) were estimated to be about 70 and 67%, respectively. The measured PL QY did not show any significant difference between pristine QDs and QDs grafted with P(NB-*r*-MA). After the phosphoric acid treatment, the PL intensity of pristine QDs significantly decreases, suggesting that CdSe@ZnS QDs are not stable in acidic condition. Under acidic treatment to remove the AAO templates, the ZnS shell layers alone could not fully protect the CdSe cores. Although the ZnS shell layer is known to be less susceptible for the surface oxidation when compared with the CdSe cores, the transformation of sulfur atoms in ZnS into sulfate ions is possible, leaving the CdSe cores vulnerable for the oxidation. The surface oxidation of QDs through a variety of pathways leads to the size reduction in QDs and concomitantly the loss of quantum efficiency.[48-51] We, however, note that QDs grafted with P(NB-*r*-MA) chains maintain their fluorescence intensity even after the treatment with phosphoric acid, as shown in Figure 3(b). The quantum efficiency of P(NB-*r*-MA)-grafted QDs decreases only by 5% after 1 h of phosphoric acid treatment. This implies that the surfaces of CdSe@ZnS QDs are well-encapsulated with norbornene copolymers and thus well protected from the acidic attack on QDs with high QY.

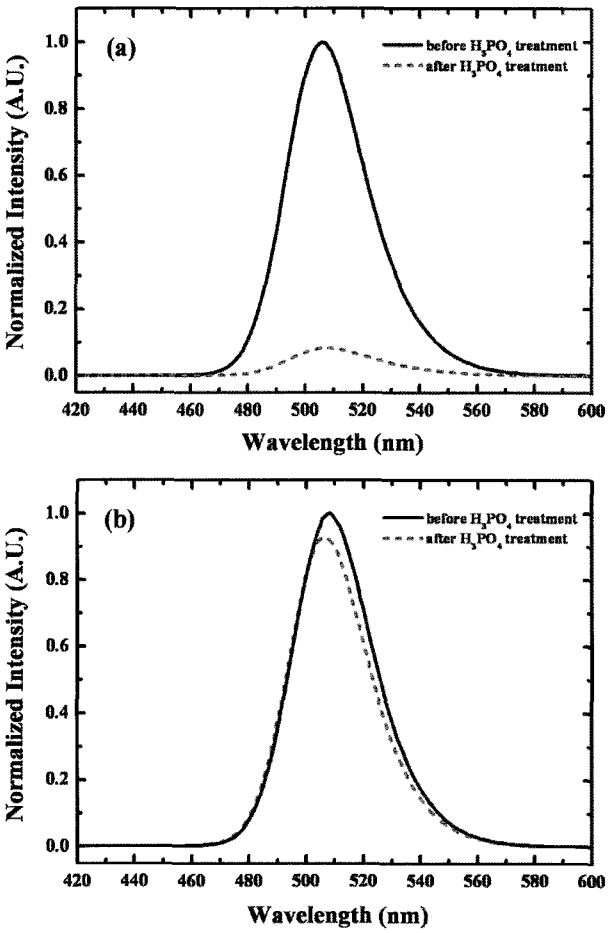

Figure 3. PL emission spectral changes of: (a) CdSe@ZnS QDs before and after the phosphoric acid treatment, (b) PNB/QD nanocomposites before and after the phosphoric acid treatment ($\lambda_{max.}$=506 nm).

Figure 4 shows photo images of pristine CdSe@ZnS QD

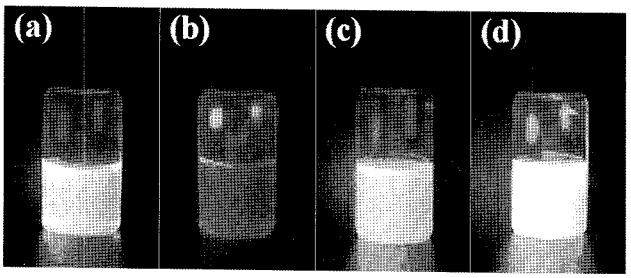

Figure 4. Photographs of (a) CdSe@ZnS QD solution, (b) CdSe @ZnS QD solution after the phosphoric acid treatment for 1 h, (c) PNB/QD nanocomposite solution, and (d) PNB/QD nanocomposite solution after the phosphoric acid treatment for 1 h.

and PNB-grafted QD solutions before and after the phosphoric acid treatment taken upon the UV irradiation at 365 nm wavelength. In Figure 4(b), the pristine QD solution almost lost its quantum efficiency upon the phosphoric acid treatment for 1 h. However, the green-emission from PNB-grafted QD solution persist even after the phosphoric acid treatment for 1 h, as shown in Figure 4(d).

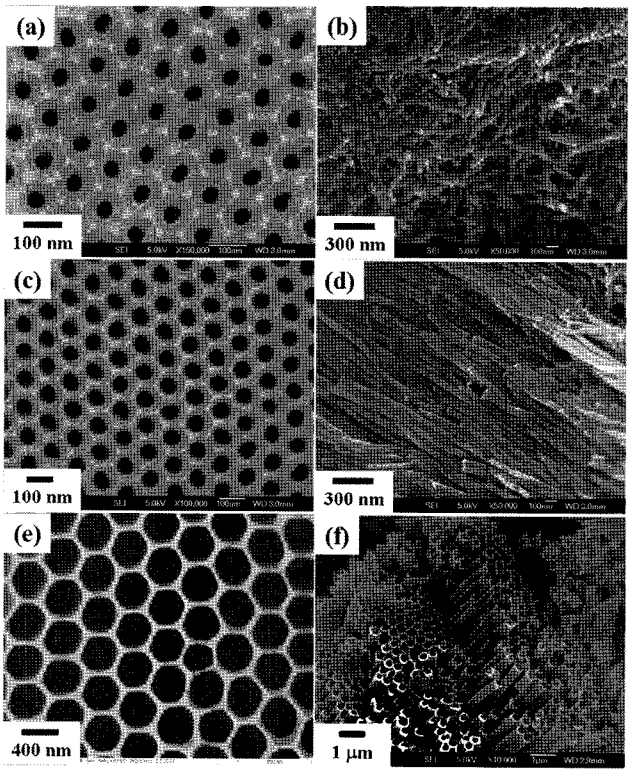

Figure 5. FE-SEM images of (a) AAO membrane with a pore diameters of 40 nm and (b) PNB/QD composite nanorods of 40 nm in diameter obtained after removing the AAO membrane; (c) AAO membrane with a pore diameters of 80 nm and (d) PNB/QD composite nanorods of 80 nm in diameter obtained after removing the AAO membrane; (e) AAO membrane with a pore diameters of 380 nm and (f) PNB/QD composite nanotubes of 380 nm in diameter obtained after removing the AAO membrane.

Image Analysis of PNB/QD Composite Nanorods and Nanotubes. AAO membranes and nanostructures of PNB/QD composites prepared from the AAO membrane templates have been examined by FE-SEM, with the results summarized in Figure 5. Well-ordered and uniform-sized AAO membranes are shown in Figures 5(a), (c), and (e). The pore size of the AAO membranes is measured as 40, 80, and 380 nm, respectively. Pore diameter and interpore distance (i.e., the center-to-center distance between neighboring pores) are controlled by experimental parameters such as type of electrolyte, applied voltage, temperature, and current during the anodization process. Usually, the interpore distance is linearly proportional to the applied voltage during the anodization step and the proportionality constant is about 2.5 nm/V. By varying the applied voltage from 25 to 195 V, we obtained well-ordered hexagonally packed pores with diameter ranging from 40 to 200 nm in the anodic aluminum oxide membranes. The pore diameter of anodic aluminum oxide membranes can be additionally tuned after the anodization by wet chemical etching, a process that enlarges the average pore diameter without altering the interpore distance and/or the membrane thickness. In this wet etch process, phosphoric acid (H_3PO_4) at 40~70 °C was typically used for the etching of aluminum oxide layer. Finally, an AAO membrane with pore size of 380 nm was successfully prepared.

Figures 5(b) and (d) show PNB/QD composite nanorods prepared from AAO membranes of different pore diameter. Furthermore, PNB/QD composite nanotubes were also obtained using the AAO membranes with larger pores. Figure

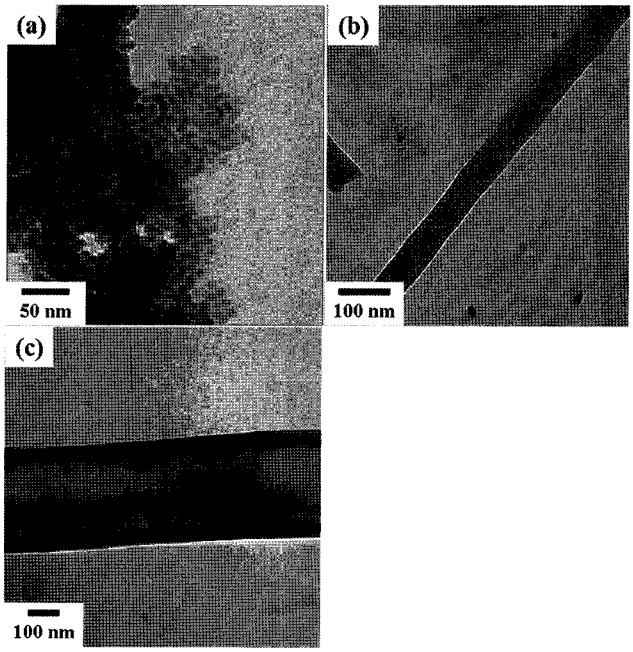

Figure 6. TEM images of (a) CdSe@ZnS QDs, (b) PNB/QD composite nanorods of 80 nm in diameter, and (c) PNB/QD composite nanotubes of 380 nm in diameter.

5(f) shows the PNB/QD composite nanotubes of 380 nm in diameter. The PNB/QD nanocomposite solution readily wets the inner surface of AAO templates with larger pores. By varying the pore size of AAO templates, we demonstrate that we could control the morphology of polymer nanocomposite structure (i.e., nanorods vs. nanotubes).

In order to obtain the detailed information on the internal structure of PNB/QD composite nanorods, TEM images were taken. Figure 6(a) shows the TEM image of CdSe@ZnS QDs used in this system. The diameter of CdSe@ZnS QDs is around 7 nm and the size distribution is fairly narrow. Figure 6(b) shows the PNB/QD composite nanorods of 80 nm in diameter, showing QDs well dispersed in the PNB matrix due to the chemical reaction between QD surface and PNB copolymer chains. Also, Figure 6(c) shows the PNB/QD composite nanotubes of 380 nm in outer diameter.

Conclusions

We have demonstrated a simple and novel approach to prepare luminescent polymer nanorods and nanotubes using AAO membrane templates of different pore size. Amine-terminated CdSe@ZnS QDs were chemically attached to capping PNB copolymers (P(NB-*r*-MA)). The QDs encapsulated with PNB copolymers were thus well protected from fluorescence quenching during the removal of AAO membranes by phosphoric acid treatment. By varying the pore size of AAO templates from 40 to 380 nm, we successfully obtained PNB/QD composite nanorods and nanotubes with QDs well-dispersed in the polymer matrix. This methodology to produce well-defined polymer/QD nanocomposites can be extended to many potential applications related to biological labeling and electro-luminescent nanomaterials.

Acknowledgments. This work was financially supported by the Korea Science and Engineering Foundation (KOSEF) grants through the Acceleration Research Program (R17-2007-059-01000-0) and the NANO Systems Institute-National Core Research Center (R15-2003-032-02002-0) funded by the Korean Ministry of Education, Science and Technology (MEST). We also acknowledge the financial support from the MEST through the Brain Korea 21 Program at Seoul National University and the International Research Training Group (IRTG) (2006-IRTG-001) Mainz-Seoul Program jointly funded by the KOSEF of Korea and the Deutsche Forschungsgemeinschaft (DFG) of Germany. Additionally, this work was supported by the World Class University (WCU) Program on the Chemical Convergence for Energy and Environment at Seoul National University (400-2008-0230).

References

(1) V. L. Colvin, M. C. Schlamp, and A. P. Alivisatos, *Nature*, **370**, 354 (1994).
(2) S. Coe, W. K. Woo, M. Bawendi, and V. Bulovic, *Nature*, **420**, 800 (2002).
(3) M. Achermann, M. A. Petruska, S. Kos, D. M. Smith, D. D. Koleske, and V. I. Klimov, *Nature*, **429**, 642 (2004).
(4) J. Lee, V. C. Sundar, J. R. Heine, and M. G. Bawendi, *Adv. Mater.*, **12**, 1102 (2000).
(5) V. I. Klimov, A. A. Mikhailovsky, S. Xu, A. Malko, J. A. Hollingsworth, C. A. Leatherdale, H. J. Eisler, and M. G. Bawendi, *Science*, **290**, 314 (2000).
(6) M. Kazes, D. Y. Lewis, Y. Ebenstein, T. Mokari, and U. Banin, *Adv. Mater.*, **14**, 317 (2002).
(7) A. V. Malko, A. A. Mikhailovsky, M. A. Petruska, J. A. Hollingsworth, H. Htoon, M. G. Bawendi, and V. I. Klimov, *Appl. Phys. Lett.*, **81**, 1303 (2002).
(8) W. U. Huynh, J. J. Dittmer, and A. P. Alivisatos, *Science*, **295**, 2425 (2002).
(9) I. Gur, N. A. Fromer, M. L. Geier, and A. P. Alivisatos, *Science*, **310**, 462 (2005).
(10) M. Bruchez, M. Moronne, P. Gin, S. Weiss, and A. P. Alivisatos, *Science*, **281**, 2013 (1998).
(11) W. C. W. Chan and S. M. Nie, *Science*, **281**, 2016 (1998).
(12) I. L. Medintz, H. T. Uyeda, E. R. Goldman, and H. Mattoussi, *Nature Materials*, **4**, 435 (2005).
(13) L. Brus, *J. Phys. Chem.*, **90**, 2555 (1986).
(14) C. B. Murray, C. R. Kagan, and M. G. Bawendi, *Annu. Rev. Mater. Sci.*, **30**, 545 (2000).
(15) A. P. Alivisatos, *Science*, **271**, 933 (1996).
(16) L. Qu and X. Peng, *J. Am. Chem. Soc.*, **124**, 2049 (2002).
(17) S. F. Wuister, A. Houselt, C. M. Donega, D. Vanmaekelbergh, and A. Meijerink, *Angew. Chem. Int. Ed.*, **43**, 3029 (2004).
(18) J. J. Li, Y. A. Wang, W. Guo, J. C. Keay, T. D. Mishima, M. B. Johnson, and X. Peng, *J. Am. Chem. Soc.*, **125**, 12567 (2003).
(19) P. Reiss, J. Bleuse, and A. Pron, *Nano Lett.*, **2**, 781 (2002).
(20) D. V. Talapin, A. L. Rogach, A. Kornowski, M. Haase, and H. Weller, *Nano Lett.*, **1**, 207 (2001).
(21) R. Xie, U. Kolb, J. Li, T. Basche, and A. Mews, *J. Am. Chem. Soc.*, **127**, 7480 (2005).
(22) Y.-K. Lee, S. M. Hong, J. S. Kim, J. H. Im, H. S. Min, E. Subramanyam, K. M. Huh, and S.-W. Park, *Macromol. Res.*, **15**, 330 (2007).
(23) C.-M. Yang, P.-H. Liu, Y.-F. Ho, C.-Y. Chiu, and K.-J. Chao, *Chem. Mater.*, **15**, 275 (2003).
(24) Y.-G. Guo, J.-S. Hu, H.-P. Liang, L.-J. Wan, and C.-L. Bai, *Chem. Mater.*, **15**, 4332 (2003).
(25) H.-S. Qian, S.-H. Yu, L.-B. Luo, J.-Y. Gong, L.-F. Fei, and X.-M. Liu, *Chem. Mater.*, **18**, 2102 (2006).
(26) C.-C. Chen, Y.-C. Liu, C.-H. Wu, C.-C. Yeh, M.-T. Su, and Y.-C. Wu, *Adv. Mater.*, **17**, 404 (2005).
(27) G.-M. Kim, A. Wutzler, H.-J. Radusch, G. H. Michler, P. Simon, R. A. Sperling, and W. J. Parak, *Chem. Mater.*, **17**, 4949 (2005).
(28) M. Lahav, T. Sehayek, A. Vaskevich, and I. Rubinstein, *Angew. Chem., Int. Ed.*, **42**, 5576 (2003).
(29) M. Bockrath, D. H. Cobden, P. L. McEuen, N. G. Chopra, A. Zettl, A. Thess, and R. E. Smalley, *Science*, **275**, 1922 (1997).
(30) A. M. Morales and C. M. Lieber, *Science*, **279**, 208 (1998).
(31) J. Jang and H. Yoon, *Adv. Mater.*, **16**, 799 (2004).
(32) K. J. Lee, J. H. Oh, Y. Kim, and J. Jang, *Chem. Mater.*, **18**,

5002 (2006).
(33) C. B. Kowollik, H. Dalton, T. P. Davis, and M. H. Stenzel, *Angew. Chem., Int. Ed.*, **42**, 3664 (2003).
(34) C. R. Martin, *Chem. Mater.*, **8**, 1739 (1996).
(35) S. Schlecht, S. Tan, M. Yosef, R. Dersch, J. H. Wendorff, Z. Jia, and A. Schaper, *Chem. Mater.*, **17**, 809 (2005).
(36) W. K. Bae, K. Char, H. Hur, and S. Lee, *Chem. Mater.*, **20**, 531 (2008).
(37) H. Masuda and K. Fukuda, *Science*, **268**, 1466 (1995).
(38) H. Masuda, F. Hasegwa, and S. Ono, *J. Electrochem. Soc.*, **144**, L127 (1997).
(39) R. H. Grubbs and W. Tumas, *Science*, **243**, 907 (1989).
(40) T. Hino and T. Endo, *Macromolecules*, **36**, 5902 (2003).
(41) C. Janiak and P. G. Lassahn, *Macromol. Rapid Commun.*, **22**, 479 (2001).
(42) S. J. Diamanti, V. Khanna, A. Hotta, D. Yamakawa, F. Shimizu, E. J. Kramer, G. H. Fredrickson, and G. C. Bazan, *J. Am. Chem. Soc.*, **126**, 10528 (2004).
(43) D. P. Sanders, E. F. Connor, and R. H. Grubbs, *Macromolecules*, **36**, 1534 (2003).
(44) J. Lipian, R. A. Mimna, J. C. Fondran, D. Yandulov, R. A. Shick, B. L. Goodall, L. F. Rhodes, and J. C. Huffman, *Macromolecules*, **35**, 8969 (2002).
(45) N. R. Grove, P. A. Kohl, S. A. Bidstrup Allen, S. Jayaraman, and R. Shich, *J. Polym. Sci. Part B: Polym. Phys.*, **37**, 3003 (1999).
(46) S. Oh, J.-K. Lee, P. Theato, and K. Char, *Chem. Mater.*, **20**, 6974 (2008).
(47) D. W. Yoo, S.-J. Yang, J.-K. Lee, J. Park, and K. Char, *Macromol. Res.*, **14**, 107 (2006).
(48) J. Aldana, Y. A. Wang, and X. Peng, *J. Am. Chem. Soc.*, **123**, 8844 (2001).
(49) V. Karabanovas, E. Zakarevicius, A. Sukackaite, G. Streckytea, and R. Rotomskis, *Photochem. Photobiol. Sci.*, **7**, 725 (2008).
(50) B. O. Dabbousi, J. Rodriguez-Viejo, F. V. Mikulec, J. R. Heine, H. Mattoussi, R. Ober, K. F. Jensen, and M. G. Bawendi, *J. Phys. Chem. B*, **101**, 9463 (1997).
(51) A. M. Derfus, W. C. W. Chan, and S. N. Bhatia, *Nano Lett.*, **4**, 11 (2004).